

Controlling continuum wavepacket interference by two-color laser field in over-the-barrier ionization regime

Sheng-Peng Zhou, Yu-Jun Yang, Da-Jun Ding[†]

Institute of Atomic and Molecular Physics, Jilin University, Changchun 130012, China

Corresponding author. E-mail: [†]dajund@jlu.edu.cn

Received August 25, 2015; accepted October 26, 2015

Continuum wavepacket interference is investigated by numerically solving the time-dependent Schrödinger equation for the interaction of hydrogen atoms with laser fields. The obtained wavepacket evolution indicates that, in the over-the-barrier ionization regime (10^{16} W/cm²), the continuum–continuum (CC) interference of ionizing electrons becomes the main process in high-order harmonics generation (HHG), compared with continuum-bound (CB) transition, as reported by Kohler *et al.* [*Phys. Rev. Lett.* 105(20), 203902 (2010)]. We propose a two-color laser field scheme for controlling the quantum trajectories of ionizing electrons and for extending the CC harmonic energy. As a result, a high energy platform occurs in the HHG spectrum, which entirely originates from the CC harmonics, with a cutoff adjustable by the relative phase of the two-color fields. This provides further understanding of the dynamic feature of atoms and molecules in super intense laser fields and provides an opportunity to image the atomic or molecular potential.

Keywords continuum–continuum interference, high-order harmonic generation, over-the-barrier ionization

PACS numbers 32.80.Fb, 42.50.Hz, 42.65.Ky

1 Introduction

High-order harmonics generation (HHG) provides a practical method for obtaining coherent short-wavelength light sources and for ultrafast determination of matter structure [1, 2]. The mechanism of the harmonics generation process can be well understood by the semi-classical three-step model [3] and its quantum interpretation [4]: atoms or molecules are ionized, the ionizing electron oscillates and gains kinetic energy in the laser field, and finally, the electron recombines with the parent ion and a harmonic photon is emitted. HHG generally occurs through a process of continuum-bound (CB) interference, the emitted photon has energy equal to the kinetic energy of the electron plus the ionization potential, and the produced HHG spectrum has a cut-off energy of $I_p + 3.2U_p$ with the ponderomotive energy $U_p = E_0^2/(4\omega^2)$ and the ionization energy I_p (E_0 and ω are the peak amplitude and frequency of the laser field, respectively). It is clear that a broad supercontinuum radiation from HHG can be generated by increasing the laser intensity for obtaining attosecond (as) opti-

cal pulses. Therefore, there has been considerable effort in investigating the interaction of super intense lasers with matter [5–10]. In the over-the-barrier ionization regime, Kohler presents a HHG mechanism through the continuum–continuum wavepacket interference (CC) for the case that the ground state is depleted, in order to generalize the traditional picture of CB harmonics [11], which is different from the case that the atom is irradiated by a laser with lower intensity [12]. In the CC process, the harmonics are generated from the interference of two continuum wavepackets in the ion potential when they recollide with the atomic core. In principal, the CC transition depends only on the shape of the potential and not on any bound state. Thus, CC harmonics have the potential for use in ultrafast imaging of atomic or molecular potential [11]. However, this strongly depends on the advancement in isolating the CC harmonics from the CB harmonics and making it dominant in the time or frequency domain.

In this paper, we theoretically investigate the HHG emission of hydrogen atoms by numerically solving the time-dependent Schrödinger equation (TDSE) in an intense laser field in the range of 10^{16} W/cm². We focus on

controlling the characteristics of CC harmonics through a two-color laser field. In Section 2 of this paper, we will briefly describe the TDSE of hydrogen atom in an intense laser field and the numerical method for solving the TDSE. In Section 3, we will analyze the HHG feature, based on a quasi-classical model of laser-induced two wavepackets interference, and investigate a method for better control of CC harmonics in the time and frequency domains by using a two-color laser field. Finally, we will summarize our results in Section 4. The study will provide further understanding of the dynamic feature of atoms and molecules in a super intense laser field and provide an opportunity for imaging the atomic or molecular potential. Throughout this paper, atomic units, a.u., $e = \hbar = m_e = 1$, are used unless otherwise

stated.

2 The theoretical model

The calculations are carried out by numerically solving a time-dependent Schrödinger equation

$$i \frac{d\psi(\mathbf{r}, t)}{dt} = \left[\frac{-1}{2} \nabla^2 + V(\mathbf{r}) - \mathbf{r} \cdot \mathbf{E}(t) \right] \psi(\mathbf{r}, t) \quad (1)$$

with the splitting operator method [13]. We use the FE-DVR to represent the kinetic and potential energy components of the Hamiltonian [14–16] and divide the matrix of the Hamiltonian into small blocks in order to ensure that the numerical computation program is parallel [17]. The electric field of the driving laser can be expressed as

$$E(t) = \begin{cases} E_0 f_0(t) \cos(\omega_0 t) & \text{(one-color)} \\ E_0 f_0(t) \cos(\omega_0 t + \phi) + E_1 f_1(t) \cos(\omega_1 t) & \text{(two-color)} \end{cases} \quad (2)$$

for one-color and two-color cases, respectively, where E_i and ω_i ($i = 0, 1$) are the peak amplitudes and frequencies of the two pulses, respectively. $\omega_0 = 0.057$ a.u. (800 nm) is the frequency of the fundamental laser field, and $\omega_1 = 0.038$ a.u. (1200 nm) is the frequency of the controlling laser field. $f_i(t) = \exp(-4 \ln 2 (t/\tau_i)^2)$ ($i = 0, 1$) are the Gaussian envelope, τ_i ($i = 0, 1$) are the pulse duration at full width of half maximum, and ϕ is the relative phase of the two lasers.

The time-dependent induced dipole acceleration is given as follows [18]:

$$\mathbf{a}(t) = -\langle \psi(\mathbf{r}, t) \left| \frac{\partial V(\mathbf{r})}{\partial \mathbf{r}} \right| \psi(\mathbf{r}, t) \rangle. \quad (3)$$

Unlike the CB case, Eq. (3) becomes $-\langle \psi_c(\mathbf{r}, t) \left| \frac{\partial V(\mathbf{r})}{\partial \mathbf{r}} \right| \psi_c(\mathbf{r}, t) \rangle$ for the CC case, which does not include any bound state and is determined by the shape of the effective potential. The information of the potential can be extracted from the CC transition [11].

The high-order harmonic spectrum $P(\omega)$ and as pulse $I(t)$ can be given by Fourier transformation of the dipole acceleration $\mathbf{a}(t)$

$$P(\omega) = \frac{1}{2\pi} \left| \int \mathbf{a}(t) e^{-i\omega t} dt \right|^2, \quad (4)$$

$$I(t) = \left| \sum_q a_q e^{i\omega t} \right|^2, \quad a_q = \int a(t) e^{-iq\omega t} dt, \quad (q = 0, 1, \dots). \quad (5)$$

For solving the 3D TDSE above, we set the time step $\Delta t = 0.005$ a.u. and the radial range from 0 to 800.0 a.u.,

which are divided into 8000 finite elements and each element contains two Gauss–Lobatto basis functions. The highest angular momentum adopted in the calculation is 1500. The computation errors give rise to the third order term in Δt [13]. It is a challenging task to solve a 3D TDSE in the case of super intense laser field up to 1.0×10^{16} W/cm². Instead, a 1D numerical model with a super-solid potential, $V(x) = -a/(|x|^{1/2} + br_B^{1/2})^2$, can be used, and the 1D TDSE can be solved by the method described in [13], where r_B is Bohr radii, the parameters are set to be $a = 1.0$ and $b = 0.6$ for matching the hydrogen ionization potential, and the space and time step are $\Delta x = 0.06$ a.u. and $\Delta t = 0.003$ a.u. This model has been successfully used for HHG calculation in a high laser intensity regime [19].

3 Results and discussion

We first investigate and compare the numerical results from 1D and 3D TDSE. Figure 1 gives the HHG spectra of hydrogen atoms in a few-cycle laser field (5 fs/800 nm, 1.0×10^{16} W/cm²) as shown in Fig. 2(a), from the 1D and 3D calculations. The shape of the platform and the cutoff energy of the two HHG spectra are the same. The widths of the as pulses obtained are almost the same when one superposes the harmonics with the energy from 9.0 to 12.0 a.u. (a width of 48 and 49 as from 1D and 3D cases, as shown in the right panels of the inset). Further, these two as pulses burst at the same time position of the laser field (near -101.0 a.u.). The only difference between the 1D and 3D results is that the peak value of

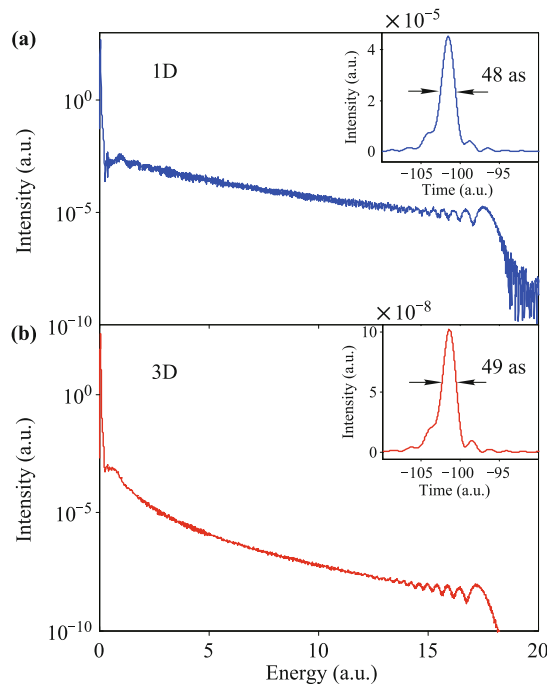


Fig. 1 HHG spectra of the hydrogen atom in a laser field (5 fs/800 nm, 1×10^{16} W/cm²) from the 1D and 3D numerical calculation. The insets are the temporal envelope of *as* pulses by superposing the HHG in the energy range of 9.0–12.0 a.u..

the *as* pulse for the 3D case is about 450 times weaker than that in the 1D case due to the larger diffusion effect of the wavepackets moving in the 3D space. Therefore, the use of the 1D super-solid model is believed to be suitable, instead of a complicated 3D model, for overcoming the difficulties of the huge computation.

Figure 2 gives the laser electric field (*E*) used in the calculation (5 fs/800 nm, 1×10^{16} W/cm²) (a), the ground state population (*P*) (b), the time-frequency analysis of HHG (c), and the evolution of the electron probability (d). In Fig. 2(c), the classical kinetic energy of the electron returning to the atomic core versus the returning time is also given by the red dashed and white dash-dotted lines, respectively, for the ionizing wavepackets produced at different half-cycles labeled A and B in (a). According to the mechanism introduced in Ref. [11], the CC harmonics is represented by the black solid line in Fig. 2(c), and its energy equals to the energy difference $|E_{kin,A} - E_{kin,B}|$ of two wavepackets returning to the core, i.e., the difference of the dashed and the dash-dotted lines. The time-frequency analysis of HHG shows that the classical and the quantum calculations are in good agreement and the CC HHG is the main process in the time duration between -50.0 and 0 a.u. It is worth noting that our numerical calculation for the evolution of the electronic probability distribution in space obviously shows this CC interference process.

As shown in Fig. 2(d), with the laser field variation, the CB interference occurs first at the time near -90.0 a.u. during the encounter between the portion of the first continuum wavepacket released in half cycle A and the bound wavepacket at the instant when the continuum wavepacket is driven back to the nuclear. This interference results in the CB harmonic emission, as given in Fig. 2(c). Then, the first continuum wavepacket moves away from the core, and the second continuum wavepacket, produced in the half cycle B, is also accelerated. Around -33.0 a.u., the two ionized wavepackets reach the nuclear simultaneously and interfere under the action of the core. This meeting of the two wavepackets near the core leads to CC harmonic emission. In fact, owing to the depletion of the ground state population after the second continuum wavepacket is released, as shown in Fig. 2(b), this CC interference becomes the main process at this moment. However, the calculated data in Fig. 2 also indicate that the CC harmonics is shielded in the total frequency spectra by the more intense CB harmonics, in the case driven by the one color laser field.

For making the CC harmonics observable in the HHG spectrum, an optimized schedule with the capability to separate the CC harmonics energy from that of CB harmonics is required. One of the possibilities is to enlarge the CC HHG platform by controlling the quantum trajectories of the electron using a two-color laser field, as widely adopted in CB HHG process [20–26]. We try to combine 800 nm/6 fs (0.9×10^{16} W/cm²) and 1200 nm/8

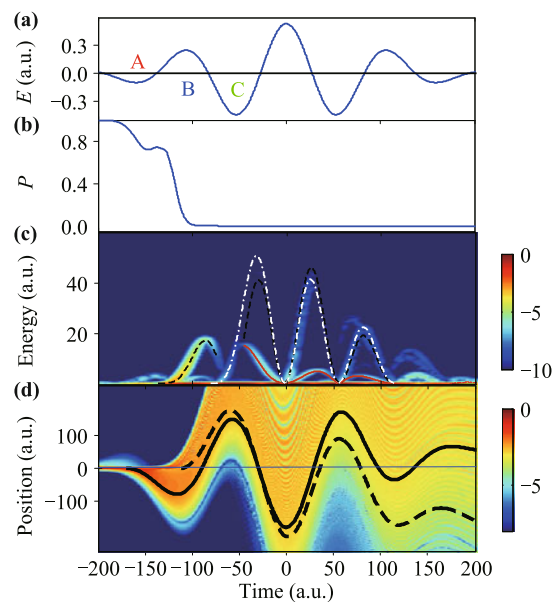


Fig. 2 (a) The two-color laser fields (6 fs/800 nm and 8 fs/1200 nm) with different relative phases of $\Phi = 0$ and 0.1π . (b) The ground state population (*P*) of the atom in the laser fields corresponding to (a). (c, d) are the HHG spectra of hydrogen atom in the laser fields.

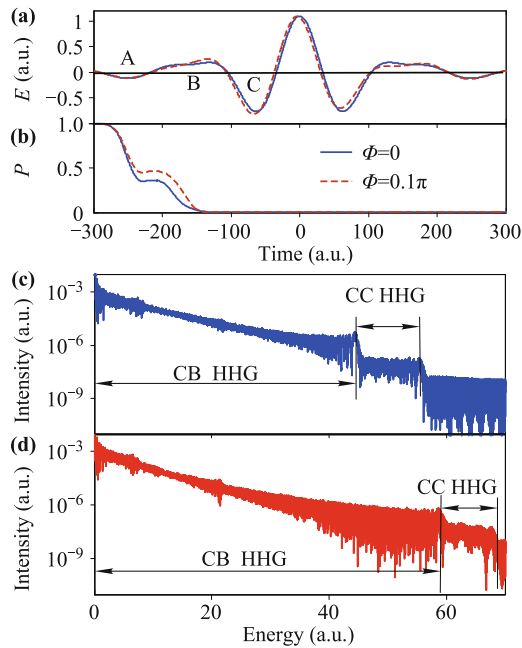


Fig. 3 The results of 1D numerical calculation for hydrogen atom in laser field. (a) The profile of the laser field (E), 5 fs/800 nm, 1×10^{16} W/cm². (b) The population of the ground state (P). (c) Time-frequency analysis of the HHG emission on a logarithmic scale. The red dashed lines and the white dash-dotted lines present the classically calculated kinetic energy of the electron return to the atomic core. The black solid lines present the difference between the dashed lines and the dash-dotted lines. (d) The evolution of the electron probability. The solid and dashed lines are the classic trajectory evolutions of the electron ionized near the peaks of two half-cycles A and B of the laser field.

fs (1.2×10^{16} W/cm²) laser fields to realize a two-color field with the profiles shown in Fig. 3(a). This profile can be varied by the relative phase $\Phi = 0$ (the solid line) and $\Phi = 0.1\pi$ (the dashed line). With the different relative phases, the calculated population P in the ground state of hydrogen atom and the HHG spectra driven by the two-color field are given in Figs. 3(b), (c) (for $\Phi = 0$), and (d) (for $\Phi = 0.1\pi$), respectively. These HHG spectra show a two-platform structure (for example, 0–45 and 45–55 a.u. for $\Phi = 0$), different from that obtained by the one-color field in which there is only one platform, as shown in Fig. 1. Like the discussion for the case of one-color field, the first platform is originated from the CB interference and the second from the CC interference, according to the time-frequency analyses shown in Fig. 4. These two-platform HHG spectra result from extending the energy of CC harmonics by controlling the quantum trajectories of the ionizing electron. We can see from the evolution of the wavepackets that the frequency spectrum is mainly affected by the electric field in three periods, as shown in Figs. 2(a) and 3(a). The electric field in different periods plays a different role. The electric field in the second and third period mainly affects

the energy of CB and CC harmonics, respectively. Thus, we can adjust the electric field in the latter two periods to influence the cutoff energies, such that the effects for the CB and CC harmonics are significantly different. For instance, to extend the CC harmonic energy to form a separated platform above the CB harmonic cutoff energy of 45 a.u. in the HHG spectrum in the two-color with relative phase 0, we considerably increase the electric field in the third period of the two-color field in the time duration of -100 to -34 a.u. [label C in Fig. 3(a)], (the absolute value of the electric field is 0.79 at the maximum, compared to that of 0.44 a.u. in the half-cycle C for the one-color laser) and slightly change the electric field in the second period.

Furthermore, controlling the HHG emission *via* CC interference in a two-color laser field is significant by varying the relative phase. Firstly, the difference of electron kinetic energy returning to the core can be controlled by changing the relative phase Φ of the two-color laser field. As shown in Fig. 3(a), the change in the relative phase from 0 to 0.1π increases the intensity of the two-color laser field from 0.19 to 0.25 a.u. in the time from -200 a.u. to -100 a.u. This results in a longer acceleration time and distance of the wavepacket ionized in this time duration before it returns to the core for the first time, and thus, the ionized wavepacket gains more kinetic energy. Correspondingly, the kinetic energy difference of the wavepackets ionized in the first two half-cycles also becomes larger when they return to the core at the same time, and which can lead to broader CC harmonics in the frequency spectrum. Figures 4(a) and (b) show that the maximum energy of the harmonics emitted at the time between -80 a.u. to 0 a.u. via CC interference is changed from 55 a.u. to 68 a.u., which is considerably broadened. Secondly, the ionization probability of two continuum wavepackets can also be controlled by the phase Φ . As shown in Fig. 3(b), according to the evolution of the ground state population P , the intensity of the continuum wavepackets ionized in the time between -300 to -217 a.u. becomes weaker and the intensity of the continuum wavepackets ionized in the time between -217 to -100 a.u. becomes stronger when the Φ changes from 0 to 0.1π . According to the CC transition expression $a_{cc} = -\langle \phi_{c1} | \nabla V | \phi_{c2} \rangle$ [11], with the two continuum wavepackets ϕ_{c1} and ϕ_{c2} . When the sum of the intensities of the two continuum wavepackets is constant, the intensities of the two wavepackets are similar, and the intensity of the CC HHG is larger. Thus, the change in the relative phase can increase the intensity of the CC harmonic spectrum. This ability to produce a broad harmonic spectrum with a certain probability from the continuum wavepackets interference can provide more

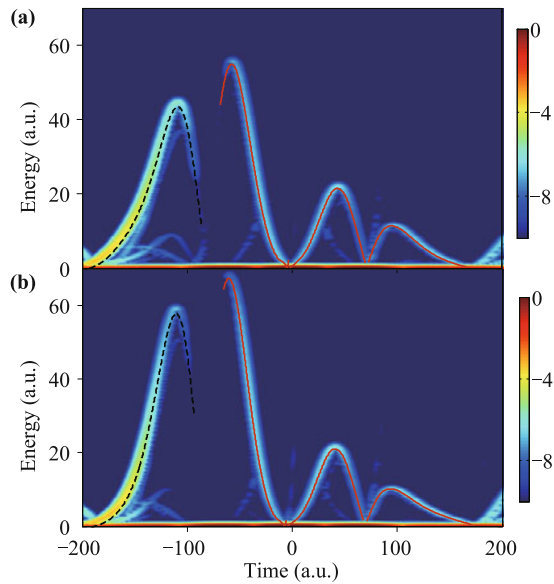


Fig. 4 Time-frequency analysis of HHG in the two-color laser field (6 fs/800 nm and 8 fs/1200 nm). The fundamental laser field is with $\Phi = 0$ (a) and $\Phi = 0.1\pi$ (b), respectively. The dashed, dash-dotted and solid lines are the classically calculated kinetic energy of the electron and their difference when returning to the core, respectively.

understanding for the atomic and molecular dynamic processes in such high laser intensity regime.

We also try to generate *as* pulses mainly from the CC harmonic spectra and analyze their characteristics since they could carry information on the potential. As expected, our calculated results show that an isolated *as* pulse can be obtained in a relatively wider phase range, compared with that from the CB process. This is because by changing the phase of a laser pulse, the local bound-state wavepacket does not change and only the nonlocal continuum wavepacket changes. Thus, the *as* pulse generation from CB interference is usually sensitive to the phase, and this influence is less influence in the case of CC interference as they do not depend on the bound state.

4 Conclusions

In conclusion, we theoretically investigate HHG via CC interference of the ionizing electron wavepacket from hydrogen atom in a strong laser field in 10^{16} W/cm². Our calculations from the perspective of the evolution of electron probability clearly show the mechanics and features of the CC interference. Based on this understanding, we propose a scheme of two-color laser field for controlling the process. By using the two-color laser field, a high energy platform from CC interference is obtained in the HHG spectrum by extending the energy of the CC har-

monics. With adjustment of the relative phase of the two-color field, the cutoff energy of this platform can be further increased, and the intensity of the CC HHG can also be enhanced as a result of the change in the ionization probability for the continuum wavepackets. The separated CC harmonics in the HHG spectrum are expected to provide an alternative method for ultrafast imaging of the molecular and atomic potentials.

Acknowledgements This work was supported by the National Basic Research Program of China (973 Program) (Grant No. 2013CB922200) and the National Natural Science Foundation of China (Grants Nos. 1127403, 11274141, and 11534004). We also acknowledge the High Performance Computing Center (HPCC) of Jilin University for supercomputer time.

References

1. C. Winterfeldt, C. Spielmann, and G. Gerber, Colloquium: Optimal control of high-harmonic generation, *Rev. Mod. Phys.* 80(1), 117 (2008)
2. J. Itatani, J. Levesque, D. Zeidler, H. Niikura, H. Pépin, J. C. Kieffer, P. B. Corkum, and D. M. Villeneuve, Tomographic imaging of molecular orbitals, *Nature* 432(7019), 867 (2004)
3. P. B. Corkum, Plasma perspective on strong field multiphoton ionization, *Phys. Rev. Lett.* 71(13), 1994 (1993)
4. M. Lewenstein, P. Balcou, M. Yu. Ivanov, A. L'Huillier, and P. B. Corkum, Theory of high-harmonic generation by low-frequency laser fields, *Phys. Rev. A* 49(3), 2117 (1994)
5. P. Moreno, L. Plaja, V. Malyshev, and L. Roso, Influence of barrier suppression in high-order harmonic generation, *Phys. Rev. A* 51(6), 4746 (1995)
6. V. V. Strelkov, A. F. Sterjantov, N. Y. Shubin, and V. T. Platonenko, XUV generation with several-cycle laser pulse in barrier-suppression regime, *J. Phys. At. Mol. Opt. Phys.* 39(3), 577 (2006)
7. J. Vazquez de Aldana and L. Roso, Magnetic-field effect in atomic ionization by intense laser fields, *Opt. Express* 5(7), 144 (1999)
8. J. A. Pérez-Hernández, L. Roso, A. Zaïr, and L. Plaja, Valley in the efficiency of the high-order harmonic yield at ultra-high laser intensities, *Opt. Express* 19(20), 19430 (2011)
9. D. Guo, C. Yu, J. Zhang, J. Gao, Z. Sun, and Z. Sun, On the cuto law of laser induced high harmonic spectra, *Front. Phys.* 10(2), 103201 (2015)
10. C. Yu, J. Zhang, Z. Sun, Z. Sun, and D. Guo, A nonperturbative quantum electrodynamic approach to the theory of laser induced high harmonic generation, *Front. Phys.* 10(4), 103202 (2015)
11. M. C. Kohler, C. Ott, P. Raith, R. Heck, I. Schlegel, C. H. Keitel, and T. Pfeifer, High harmonic generation via continuum wave-packet interferenc, *Phys. Rev. Lett.* 105(20), 203902 (2010)

12. X. Zhou and B. Li, Contribution of the bound states and continuum states of an atom in intense laser fields to high harmonic generation, *Acta Physica Sinica* 50(10), 1902 (2001) (in Chinese)
13. M. D. Feit, J. A. Jr Fleck, and A. Steiger, Solution of the Schrödinger equation by a spectral method, *J. Comput. Phys.* 47(3), 412 (1983)
14. T. N. Rescigno, and C. W. McCurdy, Numerical grid methods for quantum-mechanical scattering problems, *Phys. Rev. A* 62(3), 032706 (2000)
15. X. Guan, K. Bartschat, and B. I. Schneider, Dynamics of two-photon double ionization of helium in short intense XUV laser pulses, *Phys. Rev. A* 77(4), 043421 (2008)
16. X. Guan, K. Bartschat, and B. I. Schneider, Breakup of the aligned H₂ molecule by XUV laser pulses: A time-dependent treatment in prolate spheroidal coordinates, *Phys. Rev. A* 83(4), 043403 (2011)
17. B. I. Schneider, L. A. Collins, and S. X. Hu, Parallel solver for the time-dependent linear and nonlinear Schrödinger equation, *Phys. Rev. E* 73(3), 036708 (2006)
18. A. D. Bandrauk, S. Chelkowski, D. J. Diestler, J. Manz, and K. J. Yuan, Quantum simulation of high-order harmonic spectra of the hydrogen atom, *Phys. Rev. A* 79(2), 023403 (2009)
19. A. A. Silaev, M. Yu. Ryabikin, and N. V. Vedenkii, Strong-field phenomena caused by ultrashort laser pulses: Effective one- and two-dimensional quantum-mechanical descriptions, *Phys. Rev. A* 82(3), 033416 (2010)
20. K. Burnett, V. C. Reed, J. Cooper, and P. L. Knight, Calculation of the background emitted during high-harmonic generation, *Phys. Rev. A* 45(5), 3347 (1992)
21. S. F. Zhao, X. X. Zhou, P. C. Li, and Z. J. Chen, Isolated short attosecond pulse produced by using an intense few-cycle shaped laser and an ultraviolet attosecond pulse, *Phys. Rev. A* 78(6), 063404 (2008)
22. Y. Hong, P. X. Lu, P. F. Lan, Z. Y. Yang, Y. H. Li, and Q. Liao, Broadband xuv supercontinuum generation via controlling quantum paths by a low-frequency field, *Phys. Rev. A* 77(3), 033410 (2008)
23. Z. Zhai, R. F. Yu, X. S. Liu, and Y. J. Yang, Enhancement of high-order harmonic emission and intense sub-50-as pulse generation, *Phys. Rev. A* 78(4), 041402(R) (2008)
24. G. Chen, S. L. Liang, and Y. J. Yang, Generation of isolated sub-50-as pulses by quantum path control in the multicycle regime, *Phys. Rev. A* 82(4), 043401 (2010)
25. E. J. Takahashi, P. Lan, O. D. Mücke, Y. Nabekawa, and K. Midorikawa, Infrared two-color multicycle laser field synthesis for generating an intense attosecond pulse, *Phys. Rev. Lett.* 104(23), 233901 (2007)
26. A. Pukhov, S. Gordienko, and T. Baeva, Temporal structure of attosecond pulses from intense laser-atom interactions, *Phys. Rev. Lett.* 91(17), 173002 (2003)